doi:10.1017/S1431927622003750
Microsc. Microanal. 28 (Suppl 1), 2022
© Microscopy Society of America 2022

In-situ TEM and Spectroscopy Studies of Nanoscale Perpendicular Magnetic Tunnel Junction

Hwanhui Yun[1*], Deyuan Lyu[2], Yang Lv[2], Brandon R. Zink[2], Pravin Khanal[3], Bowei Zhou[3], Weigang Wang[3], Jian-Ping Wang[2], K. Andre Mkhoyan[1*]

[1.] Department of Chemical Engineering and Materials Science, University of Minnesota, Minneapolis, MN, United States.
[2.] Department of Electrical and Computer Engineering, University of Minnesota, Minneapolis, MN, United States
[3.] Department of Physics, University of Arizona, Tucson, AZ, United States.
[*] Corresponding authors: yunxx133@umn.edu, mkhoyan@umn.edu

Magnetic tunnel junction (MTJ), which is formed of a nonmagnetic barrier layer sandwiched between two ferromagnetic (FM) layers, is a core structure in spintronic devices. Tunneling resistance through an MTJ changes depending on magnetic configuration of the FM layers and can be controlled by applied magnetic field, current, and electric field, which can be used in various applications such as memory devices. As the structure consists of a few-nm-thick layers, well controlled growth of the stacks and following structural characterization is pivotal. While TEM has been successfully employed for the structural analysis of fabricated MTJ devices revealing the importance of the atomic and chemical configurations of each layer and the interfaces [1,2], in-situ observation of MTJ devices at the atomic-scale has not been reported yet to our best knowledge. Here, we employ in-situ electrical biasing TEM to investigate the atomic, chemical, and electronic structures of nanoscale MTJ stacks under working conditions. Perpendicular MTJ (pMTJ) [3] with magnetic easy axis in the direction normal to the film surface is studied using a Mo-buffered/capped CoFeB|MgO|CoFeB materials system, which has proven its promising properties including excellent perpendicular magnetic anisotropy, large tunnel magnetoresistance ratio, and thermal tolerance [4]. Nanopillar structured pMTJ devices with a controlled lateral dimension are fabricated, and magnetic switching is achieved by applying the electric current via spin-transfer torque [5,6]. Finally, crystalline, and chemical structural response of the device is examined via operando TEM.

pMTJ devices with a structure of Si/SiO_2 substrate\Ta(2)\Ru(6)\Ta(3)\Mo(1.2)\$Co_{20}Fe_{60}B_{20}$(1)\MgO(0.9)\$Co_{20}Fe_{60}B_{20}$(1.2-1.7)\Mo(1.9)\Ta(5)\Ru(7)\Ti/Au electrode were grown by magneton sputtering [2]. Number in the parentheses are the layer thicknesses in nm. In-situ electrical biasing TEM samples were prepared using focused ion-beam (FIB) method and mounted onto FIB-optimized E-chips (Protochips). In-situ TEM holder from Fusion Select system (Protochips) was utilized for biasing the TEM samples. STEM experiments were carried out using aberration-corrected FEI Titan G2 60-300 (S)TEM equipped with Super-X energy dispersive X-ray spectrometer for EDX and a Gatan Enfinium ER EELS.

First, structural integrity of an as-prepared pMTJ device is examined. In Fig. 1(a), a schematic of pMTJ devices used in this work is presented on the left, and a HAADF-STEM image of a nanopillar pMTJ device with a target diameter of 100 nm is displayed on the right. It was shown that a lateral dimension of the nanopillar is reduced from 100 nm at the interface with a bottom Ta electrode to ~50 nm at the top Ta/Ru electrode as marked on the HAADF-STEM image. EDX elemental maps in Fig. 1(b) clearly confirm the composition of each layer including the Mo buffer/capping layers and the

https://doi.org/10.1017/S1431927622003750 Published online by Cambridge University Press

CoFeB|MgO|CoFeB core unit, and the lattice contrast in the ABF-STEM image (Fig. 1(c)) demonstrates epitaxial growth of the crystalline layers with slightly rough interfaces. Next, I(current)-V(voltage) measurements were conducted from fabricated devices before TEM experiments. One of the devices is exemplified in Fig. 2(a) with top-down view SEM images, where a configuration of the bottom and top electrodes as well as a contrast from a nanopillar device are seen. The obtained R(Resistance)-I plot in Fig. 2(b) exhibits spin current-driven switching on/off of a pMTJ device, which is attributed to parallel/antiparallel spin directions in the two FM layers, affirming performance of the studied device. Operando TEM samples were prepared via FIB-cut of pMTJ devices such that the current flows through the pMTJ stack identical to the bulk I-V measurement. Detailed structural, compositional, and electronic configurations of the layers upon applied current are monitored via STEM imaging and EDX and EELS spectroscopies. In particular, the atomic structures, strain, and chemical diffusion at the interface and the nanopillar edge region are carefully inspected during the magnetic switching. The behavior of nanopillars with different lateral sizes range from 100 nm to 1 μm is also compared providing insight on scalability of the material system and the structure. The real time atomic-level TEM observation of nanoscale pMTJ devices will enhance our understanding of the switching behavior as well as device failure, which ultimately can be used to improve the device performance [7].

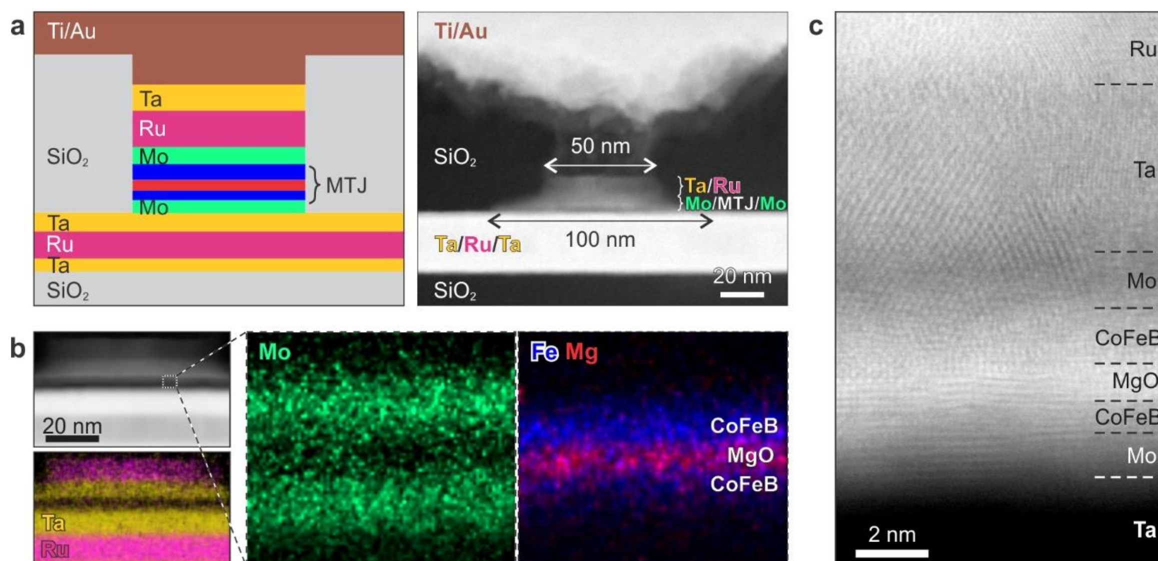

Figure 1. (a) Cross-sectional schematic (left) and a HAADF-STEM image (right) of a nanopillar structured pMTJ device. (b) EDX elemental maps showing Ta/Ru electrode layers and the core Mo|CoFeB|MgO|CoFeB|Mo stack in a nanopillar structure. (c) Atomic-resolution ABF-STEM image of the core layers.

https://doi.org/10.1017/S1431927622003750 Published online by Cambridge University Press

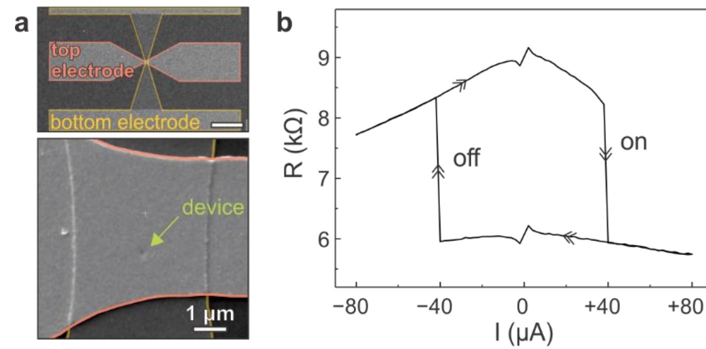

Figure 2. (a) Top-down view SEM images of a nanopillar pMTJ device with a diameter of 100 nm. The top and bottom electrode configuration is highlighted with colored outlines, and the location of nanopillar is marked. Scale bar in the top image is 50 µm. (b) Exemplary R-I curve of a 100-nm-diameter nanopillar pMTJ device.

Reference:

[1] J. J. Cha et al., Appl. Phys. Lett. **91** (2007), 062516. DOI: 10.1063/1.2769753.
[2] H. Almasi et al., Appl. Phys. Lett. **106** (2015), 182406. DOI: 10.1063/1.4919873.
[3] S. Ikeda et al., Nat. Mater. **9** (2010), 721. DOI: 10.1063/5.0066782.
[4] P. Khanal et al., Appl. Phys. Lett. **119** (2021), 242404. DOI: 10.1038/nmat2804.
[5] D. C. Worledge et al., Appl. Phys. Lett. **98** (2011), 022501. DOI: 10.1063/1.3536482.
[6] M. Gajek et al., Appl. Phys. Lett. **100** (2012), 132408. DOI: 10.1063/1.3694270.
[7] The authors acknowledge funding from SMART, one of seven centers of nCore, a Semiconductor Research corporation program, sponsored by NIST and from Defence Advanced Research Projects Agency (DARPA) FRANC program. Portions of this work were conducted in the UMN Characterization Facility supported by the NSF through the UMN MRSEC and in the Minnesota Nano Center supported by the NSF through the NNCI.

https://doi.org/10.1017/S1431927622003750 Published online by Cambridge University Press